Collective Thomson scattering model for arbitrarily drifting bi-Maxwellian velocity distributions

Abramovic, I.; Salewski, Mirko; Moseev, D.

Published in:
A I P Advances

Link to article, DOI:
10.1063/1.5088949

Publication date:
2019

Document Version
Peer reviewed version

Collective Thomson scattering model for arbitrarily drifting bi-Maxwellian velocity distributions

I. Abramovic,[1, a)] M. Salewski,[2] and D. Moseev[3]
[1)]*Eindhoven University of Technology, De Zaale, 5612 AJ Eindhoven, The Netherlands*
[2)]*Technical University of Denmark, Fysikvej, 2800 Kgs. Lyngby, Denmark*
[3)]*Max - Planck Institut fur Plasma Physik, Wendelsteinstraße 1, D-17491 Greifswald, Germany*

(Dated: 21 March 2019)

In this paper we derive the equations of collective Thomson scattering (CTS) for an arbitrarily drifting magnetized plasma described by a bi-Maxwellian distribution. The model allows the treatment of anisotropic plasma with different parallel and perpendicular temperatures (with respect to the magnetic field) as well as parallel and perpendicular plasma drift. As could be expected, parallel observation directions are most sensitive to the parallel temperature and drift, whereas perpendicular observation directions are most sensitive to the perpendicular temperature and the perpendicular drift along the observation direction. The perpendicular drift can be related to the radial electric field. Measurements with a spectral resolution better than 0.5 MHz are necessary for the inference of the radial electric field. This spectral resolution and the required scattering geometry are attainable with the current setup of the CTS diagnostic on Wendelstein 7-X.

I. INTRODUCTION

The most advanced fusion concepts, the tokamak and the stellarator, both rely on thermonuclear reactions in a magnetized plasma sustained in toroidal geometry. The plasma is heated to about 150 million degrees by fusion alphas and auxiliary heating. This extremely high temperature and the large size of fusion plasmas hamper the applicability of common plasma diagnostic methods. Microwave diagnostics, however, will work even under the conditions of future fusion reactors such as ITER or DEMO[1–3]. Collective Thomson scattering (CTS) is a microwave diagnostic based on the scattering of radiation due to fluctuations in the plasma. The incident radiation and the scattering geometry are chosen such that the condition $1/|\mathbf{k}|\lambda_{De} > 1$ is met. $\lambda_{De} = \sqrt{\frac{\varepsilon_0 T_e}{n_e e^2}}$ is the Debye length, where ε_0, T_e, n_e and e are the vacuum permittivity, electron temperature, electron density and unit charge, respectively. The scattering wave vector is defined by $\mathbf{k} = \mathbf{k}_s - \mathbf{k}_i$, where $\mathbf{k}_i$ and $\mathbf{k}_s$ represent wave vectors of the incident and scattered radiation. In this regime the scattering happens coherently on the electrons in the Debye screening clouds surrounding the ions which makes the diagnostic sensitive to the ion dynamics. This is a powerful diagnostic tool enabling simultaneous measurements of various important plasma parameters such as the ion temperature, plasma composition, drift velocity, plasma rotation, and the fast ion distribution function. In CTS one measures a spectrum of scattered radiation from which the values of the plasma parameters can be inferred. To this end a numerical forward model of the scattering has to be used.

In this paper we derive the equations of CTS for a drifting plasma described by a bi-Maxwellian distribution with arbitrary parallel drift in a perpendicularly drifting reference frame. We use our arbitrarily drifting bi-Maxwellian model to investigate the effects of anisotropic temperature as well as parallel and perpendicular drift velocities with respect to the magnetic field. The perpendicular drift velocities are related to the radial electric field, so that this important parameter can also be measured by CTS. The perpendicular plasma flow velocity and the radial electric field are linked through the force balance equation[4]

$$\langle E_r \rangle = \frac{1}{e n_i Z_i} \frac{\partial p_i}{\partial \rho} \langle \rho \rangle - \langle v_{d\perp} B \rangle \tag{1}$$

where the angle brackets denote averaging, n_i, Z_i, p_i, ρ, $v_\perp$, B are the ion density, ion charge number, ion pressure, normalized radial flux coordinate, perpendicular flow velocity and magnetic field, respectively.

Hence the value of the radial electric field can be calculated from measurements of the perpendicular flow velocity provided the other parameters are known or that the first term on the right side of equation (1) can be neglected. Diagnostics such as X-ray imaging crystal spectroscopy (XICS)[4], correlation reflectometry[5] and charge exchange recombination spectroscopy (CXRS)[6] are able to provide the measurements of the perpendicular flow velocity. However, the signal-to-noise ratio in the plasma is often low in high-density plasmas as many of the injected neutrals ionize before reaching the core. There are a number of advantages of using CTS instead. CTS directly provides local measurements and does not perturb the plasma by introducing impurities or high energy particles. It is particularly suited for high density plasma operation since the signal strength and the noise both scale with electron density and so the signal-to-noise ratio does not degrade.

We start by introducing the building blocks of our newly derived CTS model for an arbitrarily drifting bi-Maxwellian distribution function and discuss the chosen coordinate system with respect to the applied magnetic field, emphasizing the optimal scattering geometry for perpendicular drift velocity measurements (Section II). The results of the study are given in Section III. The summary and discussion outlining the implications for temperature measurements in anisotropic plasmas and for perpendicular drift velocity and radial electric

[a)]Electronic mail: i.abramovic@tue.nl

field measurements are given in Section IV. Conclusions are given in Section V.

II. CTS FOR AN ARBITRARILY DRIFTING BI-MAXWELLIAN

A. Theory

Collective Thomson scattering is the scattering of microwave radiation due to fluctuations in the plasma. The fluctuations are resolved by the measurement along the direction of $\mathbf{k}$ defined by the scattering geometry. The scattered radiation is picked up by a receiver and one measures the scattered spectral power density which is given by the transfer equation. The transfer equation can for our purposes be written in a simple form:

$$\frac{\partial P^s}{\partial \omega} = f(P^i, O_b, \omega^i, \omega^s, n_e, r_e) GS(\mathbf{k}, \omega) \tag{2}$$

where f is a function of several parameters. P_i is the probing radiation power, O_b is the overlap of the probing beam and the receiver antenna pattern, ω_i and ω_s are the frequencies of the incident and scattered waves, n_e is the electron density, and r_e is the classical electron radius. $\mathbf{k}$ and $\omega = \omega_s - \omega_i$ are associated with the fluctuations, and G and S are the dielectric and spectral form factors[7,8]. The dielectric and spectral form factors account for the response of the plasma to the incident and scattered radiation and the response of the plasma to the fluctuations interacting with the incident radiation. In what follows we will focus on these two quantities.

For probe radiation in the GHz range, the conditions for collective scattering in a fusion plasma, $1/|\mathbf{k}|\lambda_{De} > 1$, can be fulfilled while allowing for flexible scattering geometries. For waves in this range the particles in the plasma appear to be almost at rest, and the plasma can therefore be considered to be cold. The dielectric form factor G accounts for the dielectric response of the plasma to the incident and scattered radiation[9]. The cold dielectric tensor is used for the calculation of G. Treatment of the fluctuations is entirely different. The spectral form factor, or the spectral density function, $S(\mathbf{k}, \omega)$ is introduced into the CTS theory in order to account for the fluctuations in the plasma. Both of these factors are functions of the plasma parameters and the scattering geometry. In particular, the spectral density function is a function of the ion and electron velocity distributions. Radial electric field measurements by CTS require a model which is based on a suitable velocity distribution function. Given that CTS measures along the direction of $\mathbf{k}$, we also need to consider the choice of the scattering geometry such that the perpendicular plasma flow velocity is the only flow velocity which has a projection along $\mathbf{k}$. We set the coordinate system such that $v_\parallel$ refers to the velocity along the direction of the applied magnetic field $\mathbf{B}$, and the $v_{\perp 1}$ direction is in the direction of the perpendicular drift component. The bi-Maxwellian allowing for different parallel and perpendicular temperatures with respect to the magnetic field B, $T_\parallel$ and $T_\perp$, and arbitrary drifts, $v_{d\parallel}$ and $v_{d\perp}$, can then be written as[10]:

$$f^{3D}(v_\parallel, v_{\perp 1}, v_{\perp 2}) = n\Big(\frac{m}{2\pi}\Big)^{3/2} \frac{1}{T_\perp T_\parallel^{1/2}} \exp\left(- \frac{m(v_\parallel - v_{d\parallel})^2}{2T_\parallel} - \frac{m((v_{\perp 1} - v_{d\perp})^2 + v_{\perp 2}^2)}{2T_\perp} \right). \tag{3}$$

where n and m denote the particle density and mass. Parametrized in coordinates with $v_{\perp 1} = v_\perp \cos\gamma$ and $v_{\perp 2} = v_\perp \sin\gamma$, the distribution has the form:

$$f^{3D}(v_\parallel, v_\perp, \gamma) = n\Big(\frac{m}{2\pi}\Big)^{3/2} \frac{1}{T_\perp T_\parallel^{1/2}} \exp\left(- \frac{m(v_\parallel - v_{d\parallel})^2}{2T_\parallel} - \frac{m(v_\perp^2 - 2v_\perp v_{d\perp}\cos\gamma + v_{d\perp}^2)}{2T_\perp} \right) \tag{4}$$

where we do not include the Jacobian. In either coordinate system, the arbitrarily drifting bi-Maxwellian is described by three coordinates. We can see from equation (4) that any perpendicular drift breaks the axisymmetry. Symmetry breaking greatly complicates the calculation of the spectral form factor. To circumvent this problem we can restore the axisymmetry by a coordinate transformation to the guiding center frame in the perpendicular direction such that $v_{d\perp} = 0$. For $v_{d\perp} = 0$ the gyroangle γ drops out and we obtain the axisymmetric function:

$$f^{3D}(v_\parallel, v_\perp) = n\Big(\tfrac{m}{2\pi}\Big)^{3/2} \tfrac{1}{T_\perp T_\parallel^{1/2}} \exp\left(- \tfrac{m(v_\parallel - v_{d\parallel})^2}{2T_\parallel} - \tfrac{mv_\perp^2}{2T_\perp} \right) \tag{5}$$

where we can neglect the gyroangle γ in the argument since the axisymmetric function in the guiding center frame does not depend on γ. Before we proceed to calculate the spectral density function for the distribution given by (5), we also need to transform the frequencies ω to the guiding center

frame in the perpendicular direction. This transformation is advantageous as we can then use the rotation symmetric bi-Maxwellian from equation (5). The frequency shift will be due to the bulk plasma drift $\mathbf{v}_d$ and the incident probe frequency is transformed due to the moving coordinate system attached to the guiding center:

$$\omega_i' = \omega_i - \mathbf{k}_i \cdot \mathbf{v}_d \tag{6}$$

The scattered radiation frequency is also transformed due to emission from the moving coordinate system attached to the guiding center:

$$\omega_s = \omega_s' + \mathbf{k}_s \cdot \mathbf{v}_d \tag{7}$$

Assuming that the spectrum degenerates to a single line (cold plasma with T=0), we have $\omega_s' = \omega_i'$, and the scattered frequency will be:

$$\omega_s = \omega_i + \mathbf{k} \cdot \mathbf{v}_d \tag{8}$$

This is the scattering equation with the drift velocity instead of the ion velocity. The scattering is calculated for ω_s' yielding a spectrum corresponding to the shifted gyrotron frequency ω_i'. The spectrum is shifted according to equation (7). This is equivalent to the entire spectrum being shifted according to equation (8). We therefore expect to observe a systematic frequency shift ω_d given by:

$$\begin{aligned}\omega_d = \mathbf{k} \cdot \mathbf{v}_d &= k_\parallel v_{d\parallel} + k_\perp v_{d\perp} \cos\beta \\ &= k v_{d\parallel} \cos\phi + k v_{d\perp} \sin\phi \cos\beta\end{aligned} \tag{9}$$

where $k_\parallel = k\cos\phi$, $k_\perp = k\sin\phi$ and $\phi = \angle(\mathbf{k}, \mathbf{B})$. The angle β is the angle between the perpendicular drift velocity and the and the direction of $\mathbf{k}$ for a given scattering geometry[11].
The spectral density function is defined in the usual manner as the ensemble average of the Fourier-Laplace transform of the fluctuating quantity in the plasma[12]. The quantities whose fluctuations in general contribute to the CTS spectrum are the electron density, n_e, electric field, $\mathbf{E}$, magnetic field, $\mathbf{B}$, and the current density $\mathbf{j}$. Often the largest contribution comes from the electron density fluctuations which is why only these are taken into account. The spectral density function is defined as:

$$S(\mathbf{k}, \omega) = \lim_{\delta \to 0, V \to \infty} \frac{2\delta}{V} \left\langle \frac{|n_{1e}(\mathbf{k}, \omega - i\delta)|^2}{n_{0e}} \right\rangle \tag{10}$$

where V denotes the scattering volume, δ is a small positive real number (stems from the definition of the Laplace transform), n_{0e} is the mean electron density and $n_{1e}(\mathbf{k}, \omega - i\delta)$ is the Fourier-Laplace transform of the electron density fluctuations. A general expression for $S(\mathbf{k}, \omega)$ valid for arbitrary velocity distributions can be obtained provided that the Fourier-Laplace transform of the electron density fluctuations is calculated. The calculation proceeds from the Klimontovich formalism starting with the microscopic distribution function and integrating over unperturbed orbits[13]. The derivation is simplified by assuming that the plasma is collisionless and by making the electrostatic approximation. The applicability of this approximation to W7-X plasmas is discussed in[9]. The main steps in the derivation of the general expression are delineated in[12] and the final result is[12]:

$$S(\mathbf{k}, \omega) = \lim_{\delta \to 0} 2\delta \left| 1 - \frac{H_e}{\varepsilon} \right|^2 \int d\mathbf{v} \frac{\sum_{l=-\infty}^{+\infty} J_l^2(k_\perp \rho_e) f_{0e}(\mathbf{v})}{(\omega - k_\parallel v_\parallel - l\Omega_e)^2 + \delta^2} + \lim_{\delta \to 0} 2\delta Z_i^2 \left| \frac{H_e}{\varepsilon} \right|^2 \int d\mathbf{v} \frac{\sum_{l=-\infty}^{+\infty} J_l^2(k_\perp \rho_i) f_{0i}(\mathbf{v})}{(\omega - k_\parallel v_\parallel - l\Omega_i)^2 + \delta^2} \tag{11}$$

where δ is a small positive quantity, $J_l(k_\perp \rho)$ denote the Bessel functions of the first kind of order l, $\rho_{e(i)} = \frac{v_{e(i)\perp}}{\Omega_{e(i)}}$ denotes the corresponding gyroradii, $\Omega_{e(i)}$ are the corresponding cyclotron frequencies. The dispersion relation is $\varepsilon = 1 + H_e + H_i$ in which the electron and ion susceptibilities are respectively defined as[12]:

$$H_e(\mathbf{k}, \omega) = \frac{4\pi e^2 n_{0e}}{k^2 m_e} \int d\mathbf{v} \frac{\sum_{l=-\infty}^{+\infty} J_l^2(k_\perp \rho_e) \mathbf{k} \frac{\partial f_{0e}(\mathbf{k}, \mathbf{v}, \omega)}{\partial \mathbf{v}}}{\omega - i\delta - k_\parallel v_\parallel - l\Omega_e} \tag{12}$$

$$H_i(\mathbf{k}, \omega) = \frac{4\pi Z_i^2 e^2 n_{0i}}{k^2 m_i} \int d\mathbf{v} \frac{\sum_{l=-\infty}^{+\infty} J_l^2(k_\perp \rho_i) \mathbf{k} \frac{\partial f_{0i}(\mathbf{k}, \mathbf{v}, \omega)}{\partial \mathbf{v}}}{\omega - i\delta - k_\parallel v_\parallel - l\Omega_i} \tag{13}$$

where $n_{0e(i)}$ refer to the mean electron and ion densities.
The integrals in equations (11), (12) and (13) can be solved analytically for the parallel drifting bi-Maxwellian distribution function, given by equation (5), exploiting that it is separable into an integral over the ignorable gyroangle γ (the result of which is just a factor of 2π), an integral over the parallel velocity and an integral over the perpendicular velocity. For the parallel-drifting bi-Maxwellian, we have $v_{d\perp} = 0$ and hence $\omega_d = \omega_{d\parallel} = k_\parallel v_{d\parallel}$. Solving the first integral in equation (11) over the electron velocity distribution is thus broken into solving the integral over the parallel velocity:

$$\lim_{\delta \to 0} 2\delta \int_{-\infty}^{+\infty} dv_\parallel \frac{e^{-\frac{m_e (v_\parallel - v_{d\parallel})^2}{2T_{e\parallel}}}}{(\omega - k_\parallel v_\parallel - l\Omega_e)^2 + \delta^2} = \frac{2\pi}{k_\parallel} e^{-\left(\frac{\omega - \omega_{d\parallel} - l\Omega_e}{v_{t\parallel e} k_\parallel}\right)^2} \tag{14}$$

and the integral over the perpendicular velocity:

$$C\int_0^{+\infty} v_\perp dv_\perp \sum_{l=-\infty}^{+\infty} J_l^2(k_\perp\rho_e)e^{-\frac{m_e v_\perp^2}{2T_{e\perp}}} = C\frac{T_{e\perp}}{m_e}\sum_{l=-\infty}^{+\infty} e^{-\left(\frac{k_\perp^2 T_{e\perp}}{\Omega_e^2 m_e}\right)} I_l\Big(\frac{k_\perp^2 T_{e\perp}}{\Omega_e^2 m_e}\Big) \tag{15}$$

where $C = (\frac{m_e}{2\pi})^{3/2}\frac{1}{T_{e\perp}T_{e\|}^{1/2}}$, and we used the following property of the Bessel function of the first kind for calculating the integral over the perpendicular velocity[14]:

$$\int_0^{+\infty} J_l^2(bt)e^{-p^2t^2}tdt = \frac{1}{2p^2}e^{-\left(\frac{b^2}{2p^2}\right)} I_l\Big(\frac{b^2}{2p^2}\Big) \tag{16}$$

Collecting the terms from (14)-(16) we find the result of the integral from equation (11) over the electron velocity distribution. The integral over the ion velocity distribution from equation (11) can be completed in an analogous manner. The resulting spectral density function is:

$$S(\mathbf{k},\omega) = \left|1-\frac{H_e}{\varepsilon}\right|^2 \frac{2\pi^{1/2}}{v_{t\|e}k_\|}\sum_{l=-\infty}^{+\infty} e^{-\left(\frac{k_\perp^2 T_{e\perp}}{\Omega_e^2 m_e}\right)} I_l\Big(\frac{k_\perp^2 T_{e\perp}}{\Omega_e^2 m_e}\Big) e^{-\left(\frac{\omega-\omega_{d\|}-l\Omega_e}{v_{t\|e}k_\|}\right)^2} + \left|\frac{H_e}{\varepsilon}\right|^2 \frac{2\pi^{1/2}Z_i^2 n_i}{n_e v_{t\|i}k_\|}\sum_{l=-\infty}^{+\infty} e^{-\left(\frac{k_\perp^2 T_{i\perp}}{\Omega_i^2 m_i}\right)} I_l\Big(\frac{k_\perp^2 T_{i\perp}}{\Omega_i^2 m_i}\Big) e^{-\left(\frac{\omega-\omega_{d\|}-l\Omega_i}{v_{t\|i}k_\|}\right)^2} \tag{17}$$

where $v_{t\|e} = \sqrt{\frac{2T_{e\|}}{m_e}}$, $v_{t\|i} = \sqrt{\frac{2T_{i\|}}{m_i}}$. The derived expression for the spectral density function given by equation (17) is valid for single ion species plasma but can easily be generalized to multiple ion species plasma by summation of the second term over all ion species.

Calculations of the integrals from equations (12) and (13) require the use of the definition of the plasma dispersion function[15]

$$Z(\eta) = \frac{1}{\sqrt{\pi}}\int_{-\infty}^{+\infty} dx\frac{e^{-x^2}}{x-\eta} \tag{18}$$

and the following recurrence relation for Bessel functions of the first kind[14]

$$J_{l-1}(z) + J_{l+1}(z) = \frac{2l}{z}J_l(z) \tag{19}$$

The relation (19) enables writing out the product of the wave vector and the partial derivative of the distribution function in the following form[12]

$$\mathbf{k}\frac{\partial f_{0e}}{\partial \mathbf{v}} = k_\|\frac{\partial f_{0e}}{\partial v_\|} + \frac{l\Omega_e}{v_\perp}\frac{\partial f_{0e}}{\partial v_\perp} \tag{20}$$

After the calculation we get the final expressions for the susceptibilities:

$$H_e = \frac{1}{k^2\lambda_{De\|}^2}\sum_{l=-\infty}^{\infty} e^{-\left(\frac{k_\perp^2 T_{e\perp}}{\Omega_e^2 m_e}\right)} I_l\Big(\frac{k_\perp^2 T_{e\perp}}{\Omega_e^2 m_e}\Big)\left(1+\frac{\omega-\omega_{d\|}}{v_{t\|e}k_\|}Z\Big(\frac{\omega-\omega_{d\|}-l\Omega_e}{v_{t\|e}k_\|}\Big)\right) \tag{21}$$

$$H_i = \frac{Z_i^2 T_{e\|} n_i}{k^2\lambda_{De\|}^2 T_{i\|} n_e}\sum_{l=-\infty}^{\infty} e^{-\left(\frac{k_\perp^2 T_{i\perp}}{\Omega_i^2 m_i}\right)} I_l\Big(\frac{k_\perp^2 T_{i\perp}}{\Omega_i^2 m_i}\Big)\left(1+\frac{\omega-\omega_{d\|}}{v_{t\|i}k_\|}Z\Big(\frac{\omega-\omega_{d\|}-l\Omega_i}{v_{t\|i}k_\|}\Big)\right) \tag{22}$$

From the obtained expression it follows that the plasma drift will cause a frequency shift of the measured spectra which is in accordance with expectations based on rotation measurements by CTS described in[16]. The usual expressions for the isotropic Maxwellian distribution without drifts can be recovered by setting $T_\perp = T_\|$ and $\omega_d = 0$ in equations (17), (21) and (22).

For electric field measurements we need to make sure that the frequency shift is caused only by the perpendicular drift velocity. This is accomplished by choosing the scattering geometry such that $\angle(\mathbf{k},\mathbf{B}) = \pi/2$ so that $k_\| = 0$. This is a very convenient geometry also due to the possibility of observing the cyclotron signature in measured CTS spectra[16]. The peaks in the spectra appear near the cyclotron frequencies of the ions in the plasma. These features are very narrow and thus improve the spectral resolution crucial for resolving the frequency shift caused by the radial electric field. If we consider the angle β between the perpendicular drift velocity and the line of sight, the frequency shift will be given by $kv_{d\perp}\cos\beta$ for the $\phi = 90$ case. If two simultaneous measurements on the same overlap volume are available, one can recover all the parameters of the underlying bi-Maxwellian distribution function.

Since the spectral shift of the cyclotron signature does not depend on the number of fluctuating quantities taken into account, or effects captured by a full electromagnetic treatment, it will suffice to calculate the spectral density function in the electrostatic approximation accounting only for the fluctuations in the electron density.

B. Computation

A forward model enabling numerical computation of collective Thomson scattering spectra (eCTS) has been developed and described in[9]. The eCTS code is based on the electrostatic approximation which suffices for modeling the bulk ion feature in CTS spectra, as well as inference of plasma composition and drift velocities. The code has extensively been bench-marked against a full electromagnetic model[17] with which an agreement within 10% is found for isotropic Maxwellian plasmas[9]. The model has also been validated on Wendelstein 7-X and the data analysis procedure is described in[18]. The model takes as input the values of plasma and scattering geometry parameters and calculates the spectral power density of the scattered radiation given by the transfer equation (2). To investigate the effects of anisotropic temperatures and to study the feasibility of radial electric field measurements in Maxwellian and bi-Maxwellian plasma, we have extended the eCTS model by implementing a spectral density function calculated for a distribution given by equation (5).

III. RESULTS

A. Sensitivity to Anisotropic Ion Temperatures $T_\perp$ and $T_\parallel$

By resolving the plasma fluctuations along the direction $\mathbf{k}$, the CTS diagnostic measures a projection of the ion velocity distribution function along this direction. The spectrum is therefore highly sensitive to the changes in the observation angle $\phi = \angle(\mathbf{k}, \mathbf{B})$ for anisotropic velocity distribution functions. We calculated spectra for the three observation angles $\phi = 10^\circ$, $\phi = 80^\circ$ and $\phi = 90^\circ$ and for each case, we investigated the effects of changing the parallel and perpendicular temperatures. The results are depicted in Figures 1, 2 and 3, respectively. Similar to the case for an isotropic Maxwellian distribution, we expect that an increase in ion temperature will in general affect the width of the spectra. For our model which calculates CTS in a bi-Maxwellian plasma the observation angle determines to which of the two temperatures, $T_\perp$ or $T_\parallel$, the width is more sensitive to. By comparing Figures 1 and 2 we conclude that in the first case for $\phi = 10^\circ$ the width of the spectrum is dominated by the change in $T_\parallel$, whereas in the second case for $\phi = 80^\circ$ the width is dominated by the change in $T_\perp$. This angular dependence is strongly modified by the appearance of ion cyclotron signatures for angles near $\phi = 90^\circ$ - the sharp peaks depicted in Figure 3 which correspond to the ion cyclotron frequency. The onset of the ion cyclotron signature is gradual as we approach perpendicular observation. This is shown in Figure 4 in which the observation angle is systematically varied from $\phi = 85^\circ$ up to $\phi = 89^\circ$. In experiments, notch filters block a spectral range around the probing frequency (± 150 MHz) in order to protect the sensitive CTS receiver from high power radiation. In Figure 4 an ideal notch filter region is indicated. In practice the notch does not have ideal characteristics and the actual range within which the signal is gradually attenuated can be significantly wider. This increases the uncertainty of the height of CTS spectra in an actual measurement. Additionally the height also scales with a number of parameters such as the incident power, the overlap volume, the electron density, and the dielectric form factor (see equation 1). All the parameters to which the spectrum is sensitive but which are not to be inferred from a CTS measurement we refer to as the nuisance parameters. The sensitivity of calculated CTS spectra to nuisance parameters has been investigated for the isotropic Maxwellian case in[18].

B. Sensitivity to Plasma Drift

Changes in the values of plasma parameters such as the ion and electron temperatures and densities, the applied magnetic field and the scattering angle, affect both the height and the width of the calculated spectra[18]. The impurity concentrations, reflected in the value of effective charge Z_{eff}, can distort the spectral shape for high concentrations of lighter impurities such as helium or carbon[19]. Depending on the value of the projection angle ϕ, the diagnostic can be made sensitive to the plasma composition which can be inferred from the ion cyclotron signature observable under the condition of perpendicular observation[20] and as depicted in Figure 3. However, changes in plasma parameters and scattering geometry will not affect the centering of the spectrum around the probing frequency. Thus the only quantity causing a spectral shift of CTS spectra will be a drift velocity.

We in particular seek to infer the perpendicular drift velocity. As discussed the parallel drift velocity drops out for $\phi = 90^\circ$, and the frequency shift in the spectra remains small for angles close to 90°. The radial electric field can be calculated from the equation (1) provided the perpendicular drift velocity can be inferred from measured CTS spectra. This in practice translates into the requirement that the frequency shift be resolvable. To investigate if this is the case, we need to calculate the spectra within a relevant parameter range and find the necessary spectral resolution of our CTS diagnostic and thus the feasibility of using it for radial electric field measurements. In the first experimental campaign of Wendelstein 7-X, the average perpendicular flow velocity was measured by the XICS diagnostic and corresponding values of the radial electric field have been obtained[4]. We therefore chose to conduct our study for similar plasma parameter values from 2 kV/m up to 12 kV/m as reported in[4], for a conveniently chosen scattering geometry - perpendicular observation $\phi = 90^\circ$. Relevant ranges of input parameters are summarized in Table 1. We have systematically changed the input values of $\mathbf{v}_d$ in order to quantify the corresponding frequency shift. Changes in the value of the drift velocity, taken such as to correspond to the values of the radial electric field from 2 kV/m up to 12 kV/m,

Parameter	Range
T_e [keV]	2 - 7
T_i [keV]	1 - 5
n_e $10^{19}m^{-3}$	2 - 8
n_i $10^{19}m^{-3}$	2 - 8
Z_{eff}	1 - 2
B [T]	2.34
$\phi = \angle(\mathbf{k}^{\delta}, \mathbf{B})$ [deg]	88 - 90
$\theta = \angle(\mathbf{k}_i, \mathbf{k}_s)$ [deg]	150 - 170

TABLE I. Parameter ranges for the feasibility study of radial electric field measurements by CTS

cause spectral shifts of 0.35 MHz up to 4.25 MHz. A calculation of the largest shift for perpendicular observation is shown in Figure 5. The spectral shift can be calculated from a spectrum containing the ion cyclotron signature in two ways: by fitting the measured spectra with our model or by simply finding the shift of the peaks and minima. Using the model has the advantage that all data points are used in the fit. However, uncertainties in nuisance parameters may complicate this approach. The approach to simply find the frequency shift of the peaks exploits the symmetry of the ion cyclotron signature about the probe frequency. The frequency shift can be calculated by summing the frequencies of the corresponding peaks on the left and the right side of the incident frequency. If such peaks are identifiable in a measurement, one pair of frequencies will suffice for the calculation of the shift which will simply be given by:

$$\Delta\omega = \frac{\omega_{right} + \omega_{left}}{2} - \omega_i \tag{23}$$

where ω_i stands for the frequency of the probing radiation. In order to decrease the noise we should use all identifiable peak and minimum pairs by summing over frequencies:

$$\Delta\omega = \sum_{n=1}^{N} \frac{\omega_{n_{right}} + \omega_{n_{left}}}{2N} - \omega_i \tag{24}$$

where N denotes the number of identifiable peak pairs and minimum pairs.

For observation other than perpendicular, the parallel drift velocity will contribute to the observed spectral shift. Computing the spectra for parallel drift velocities at $\phi = 0^\circ$ and $\phi = 60^\circ$ are shown in Figure 6. As can be seen from Figure 6 the spectral resolution relative to the frequency shift caused by the parallel drift velocity is larger at smaller ϕ. This makes it easier to measure parallel drift for more parallel observation.

It should be emphasized that there are two ways of computing the shifted spectra, namely by using the equations (6)-(8), and by using equations (17), (21), (22) resulting from a formal derivation or by applying the spectral-shift method (shifting the spectrum for $\mathbf{v_d} = 0$ by $\mathbf{k} \cdot \mathbf{v_d}$). The two methods have been applied to the calculation of spectra in Figure 6 confirming that the two are equivalent. The calculation of the perpendicular drift can only be handled by the spectrum-shift method since we need to retain the rotational symmetry.

IV. SUMMARY AND DISCUSSION

In this work we have derived the equations enabling us to calculate CTS spectra for a plasma described by a bi-Maxwellian distribution function with arbitrary parallel drift in a perpendicularly drifting reference frame. The equations were incorporated into the forward model of CTS in the electrostatic approximation eCTS described in[9]. This further allowed investigation of two topics: first, the effects of anisotropic temperatures, $T_\perp$ and $T_\parallel$, as well as perpendicular and parallel drifts, $v_{d\perp}$ and $v_{d\parallel}$, on CTS spectra in magnetized high-temperature plasmas with bi-Maxwellian distributions and the investigation of the feasibility of radial electric field measurements in such plasmas. We have shown that the width of CTS spectra calculated for a bi-Maxwellian plasma is affected by the changes in both $T_\perp$ and $T_\parallel$. Depending on the chosen observation angle ϕ the width is more sensitive to either $T_\perp$ or $T_\parallel$. This is in agreement with expectations based on the projection equations for bi-Maxwellian plasma given in[11] where it is shown that the $T_\perp$ and $T_\parallel$ drop out in the projection of the velocity distribution function onto the line-of-sight (here $\mathbf{k}$) for the limiting cases of $\phi = 0^\circ$ and $\phi = 90^\circ$, respectively. However, for $\phi = 90^\circ$ the appearance of the ion cyclotron signature modifies the expected dependence on the perpendicular and parallel temperatures and the sensitivity to $T_\parallel$ is retained, as can be seen in Figure 3. This has implications for the inference of bulk ion temperature from CTS spectra. Therefore, if powerful NBI or ICRF heating is employed in low-density plasma, accounting for anisotropy could be essential for a correct interpretation of the measurements.

For the measurements of small spectral shifts from which E_r can be determined, high resolution and a narrow notch filter are required. The notch filter can be very narrow (up to 10 MHz) provided the gyrotron frequency is stable[21]. This will enable observation of the ion cyclotron signature even for narrow spectra. If a narrow notch filter is not available, we will benefit from heating scenarios such that $T_\perp > T_\parallel$ in which we expect spectral broadening for close to perpendicular observation as illustrated in Figure 3.

The spectral resolution in modern CTS DAQ systems, such as the ones employed on Wendelstein 7-X[22] and AUG[23], is flexible. The receiver samples with the rate of 5-12 GS/s. A Fourier transform is made in order to obtain the scattering spectrum and the spectral resolution is then given by 1/T where T stands for the duration of the acquisition period. This allows for a high spectral resolution better than 1 MHz. The limiting factor can be background subtraction. Nevertheless, provided that the right scattering geometry and forward model are used, the measurement of the radial electric field by means of CTS is feasible.

V. CONCLUSION

The forward model based on the herein outlined equations (17), (21) and (22) should be used for interpretation of CTS measurements in drifting bi-Maxwellian plasmas produced by NBI or ICRH heating in which the anisotropy in temperature

has to be taken into account. The model formalizes the intuitive interpretation of spectral shifts in CTS measurements by explicitly relating the shifts to plasma drift velocities. We have demonstrated that perpendicular observation in conjunction with the relation given by equation (24) can be used for perpendicular drifts measurements from which the radial electric field can be inferred. The CTS can thus provide the radial electric field values in plasmas where impurity based diagnostics would be hampered by the large plasma volume and density.

ACKNOWLEDGEMENTS

The corresponding author would like to thank Prof. Dr. Niek J. Lopes Cardozo for insightful inputs and support.
This work has been carried out within the framework of the EUROfusion Consortium and has received funding from the Euratom research and training programme 2014-2018 and 2019-2020 under grant agreement No 633053. The views and opinions expressed herein do not necessarily reflect those of the European Commission.

REFERENCES

[1] F. Volpe, *Prospects for a dominantly microwave-diagnosed magnetically confined fusion reactor*, JINST, Vol 12 (01), C01094 (2017)
[2] D. Moseev, M. Salewski, M. Garcia-Muñoz, B. Geiger, M. Nocente, Rev. Mod. Plasma Phys. (2018) 2:7
[3] M. Salewski, M. Nocente, B. Madsen, I. Abramovic, M. Fitzgerald, G. Gorini, P.C. Hansen, W.W. Heidbrink, A.S. Jacobsen, T. Jensen et al., (2018) Nucl. Fusion 58 096019
[4] N. A. Pablant, A. Langenberg, A. Alonso, C. D. Beidler, M. Bitter, S. Bozhenkov, R. Burhenn, M. Beurskens, L. Delgado-Aparicio, A. Dinklage et al., *Core radial electric field and transport in Wendelstein 7-X plasmas*, Physics of Plasmas 25, 022508, (2018)
[5] T. Windisch, A. Krämer-Flecken, J. L. Velasco, A. Könies, C. Nührenberg, O. Grulke, T. Klinger and the W7-X team, *Poloidal correlation reflectometry at W7-X: radial electric field and coherent fluctuations*, Plasma Phys. Control. Fusion 59 (10), 105002 (2017)
[6] J. W. Coenen, B. Schweer, M. Clever, S. Freutel, O. Schmitz, H. Stoschus, U. Samm and B. Unterberg, *Charge exchange recombination spectroscopy on a diagnostic hydrogen beam-measuring impurity rotation and radial electric field at the tokamak TEXTOR*, J. Phys. B: At. Mol. Opt. Phys. 43 (14), 144015 (2010)
[7] T. Hughes, S. Smith, *Effects of plasma dielectric properties on Thomson scattering of millimetre waves in tokamak plasmas*, Journal of Plasma Physics 42 (2), 215-240 (1989)
[8] T. Hughes, S. Smith, *Calculations of Thomson scattering functions for alpha particle diagnostics in JET plasmas*, Nuclear Fusion 28 (8), 1451 (1988)
[9] I. Abramovic, A. Pavone, D. Moseev, N. J. Lopes Cardozo, M. Salewski, H. P. Laqua, M. Stejner, T. Stange, S. Marsen, S. K. Nielsen et al., *Forward Modeling of Collective Thomson Scattering for Wendelstein 7 - X Plasmas: Electrostatic Approximation*, Rev. Sci. Instrum. 90, 023501 (2019); https://doi.org/10.1063/1.5048361
[10] D. Moseev and M. Salewski, *Bi-Maxwellian, slowing-down, and ring velocity distributions of fast ions in magnetized plasmas*, Phys. Plasmas 26, 020901 (2019); doi: 10.1063/1.5085429
[11] M. Salewski, B. Geiger, A.S. Jacobsen, I. Abramovic, S.B. Korsholm, F. Leipold, B. Madsen, J. Madsen, R.M. McDermott, D. Moseev, S.K. Nielsen et al., *Deuterium temperature, rotation and density measurements in non-Maxwellian plasmas at ASDEX Upgrade*, Nuclear Fusion 58, 036017 (2018)
[12] J. Sheffield, D. Froula, Siegfried H. Glenzer, Neville C. Luhmann, Jr., *Plasma Scattering of Electromagnetic Radiation*, Academic Press (2010)
[13] YU. L. Klimontovich, *The Statistical Theory of Non-Equilibrium Processes in a Plasma*, Pergamon Press Ltd., 1967
[14] M. Abramowitz, I. Stegun, *Handbook of Mathematical Functions with Formulas, Graphs, and Mathematical Tables*, Wiley Interscience, NY, (1972)
[15] B. Fried, S, Conte, *The Plasma Dispersion Function*, Academic Press, NY, (1961)
[16] M. Stejner, S. K. Nielsen, A. S. Jacobsen, S. B. Korsholm, F. Leipold, R. M. McDermott, P. K. Michelsen, J. Rasmussen, M. Salewski, M. Schubert et al., *Plasma rotation and ion temperature measurements by collective Thomson scattering at ASDEX Upgrade*, Plasma Physics and Controlled Fusion, Volume 57 (6), 062001 (2015)
[17] H. Bindslev, *A quantitative study of scattering from electromagnetic fluctuations in plasmas*, Journal of Atmospheric and Terrestrial Physics 58 (1996), Nos. 8/9
[18] I. Abramovic, A. Pavone, J. Svensson, D. Moseev, M. Salewski, H.P. Laqua, N.J. Lopes Cardozo and R.C. Wolf, *Collective Thomson scattering data analysis for Wendelstein 7-X*, JINST 12 (8), C08015 (2017)
[19] M. Salewski, F. Meo, M. Stejner, O. Asunta, H. Bindslev, V. Furtula, S.B. Korsholm, T. Kurki-Suonio, F. Leipold, F. Leuterer et al., *Comparison of fast ion collective Thomson scattering measurements at ASDEX Upgrade with numerical simulations*, Nucl. Fusion 50 (2010) 035012
[20] M. Stejner, S. B. Korsholm, S. K. Nielsen, M. Salewski, H. Bindslev, S. Brezinsek, V. Furtula, F. Leipold, P. K. Michelsen, F. Meo et al., *Measurements of plasma composition in the TEXTOR tokamak by collective Thomson scattering*, Plasma Phys. Control. Fusion 54, 015008 (2012)

[21] A. Fokin, M. Glyavin, G. Golubiatnikov, L. Lubyako, M. Morozkin, B. Movschevich, A. Tsvetkov and G. Denisov, *High-power sub-terahertz source with a record frequency stability at up to 1 Hz*, Nature Scientific Reports, 4317 (2018)

[22] D. Moseev, M. Stejner, T. Stange, I. Abramovic, H. P. Laqua, S. Marsen, N. Schneider, H. Braune, U. Hoefel, W. Kasparek, S. B. Korsholm et al., *Collective Thomson Scattering Diagnostic on Wendelstein 7-X*, Review of Scientific Instruments 90, 013503 (2019)

[23] V. Furtula, F. Leipold, M. Salewski, P. K. Michelsen, S. B. Korsholm, F. Meo, D. Moseev, S. K. Nielsen, M. Stejner and T. Johansen, *Performance measurements of the collective Thomson scattering receiver at ASDEX Upgrade*, Journal of Instrumentation 7 (02), C02039 (2012)

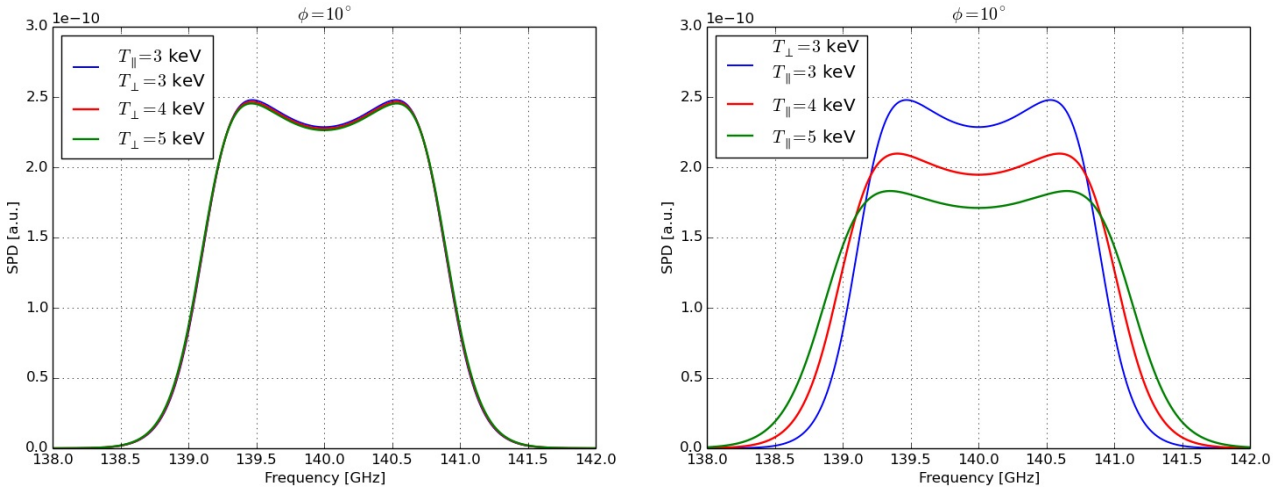

FIG. 1. Variation of $T_\perp$ (left) and $T_\parallel$ (right) for a fixed observation angle of $\phi = 10^\circ$, showing that for more parallel observation the width of CTS spectra is more sensitive to changes in $T_\parallel$.

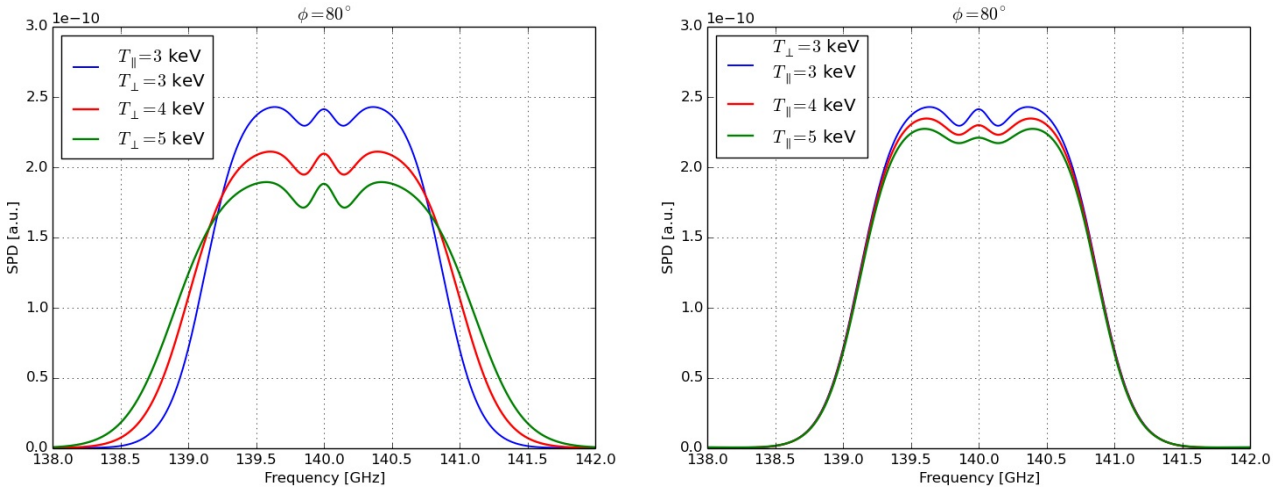

FIG. 2. Variation of $T_\perp$ (left) and $T_\parallel$ (right) for a fixed observation angle of $\phi = 80^\circ$, showing that for more perpendicular observation the spectral width becomes more sensitive to the changes in $T_\perp$.

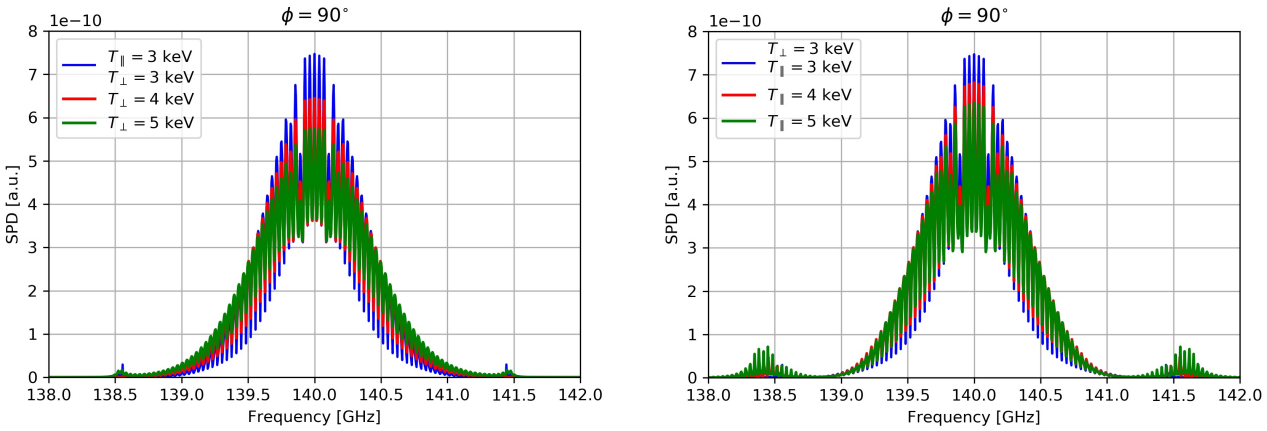

FIG. 3. Variation of $T_\perp$ (left) and $T_\parallel$ (right) for a fixed observation angle of $\phi = 90^\circ$. For this observation angle we expect, taking into account the results depicted in Figures 1 and 2, that the spectral width reflects the changes in $T_\perp$. This dependence is made less obvious due to the appearance of sharp peaks in the spectra which correspond to the cyclotron frequency of the ions - appearance of the ion cyclotron signature.

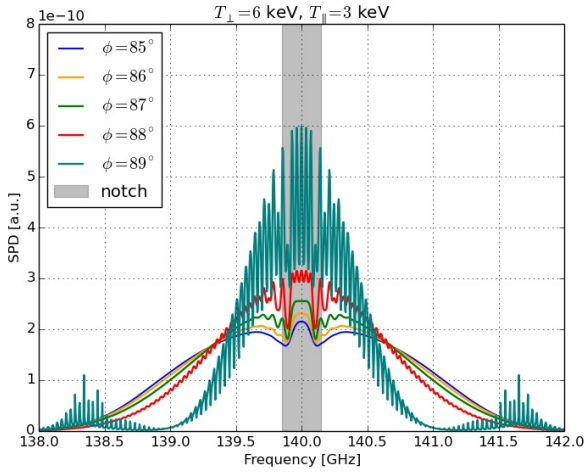

FIG. 4. Gradual onset of ion cyclotron signature as ϕ approaches 90° with indicated notch filter region.

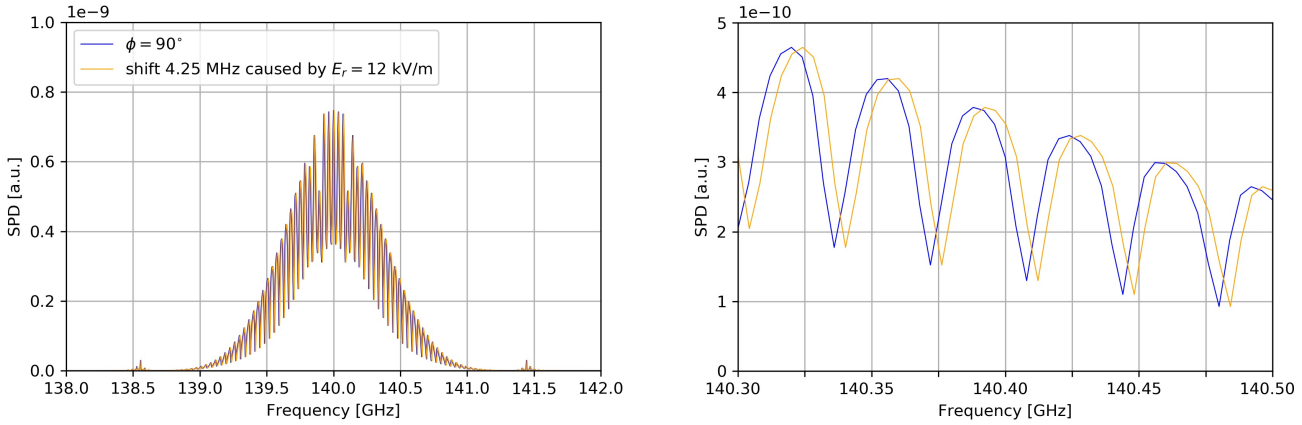

FIG. 5. Calculation of the spectral shift of a CTS spectrum caused by the radial electric field in the scattering volume of a Maxwellian hydrogen plasma. On the left: the spectrum has been calculated for perpendicular observation. The cyclotron signature is clearly visible (peaks in the spectrum). On the right: enlarged part of the spectrum, the calculated frequency shift of 4.25 MHz corresponds to a field of $E_r = 12$ kV/m

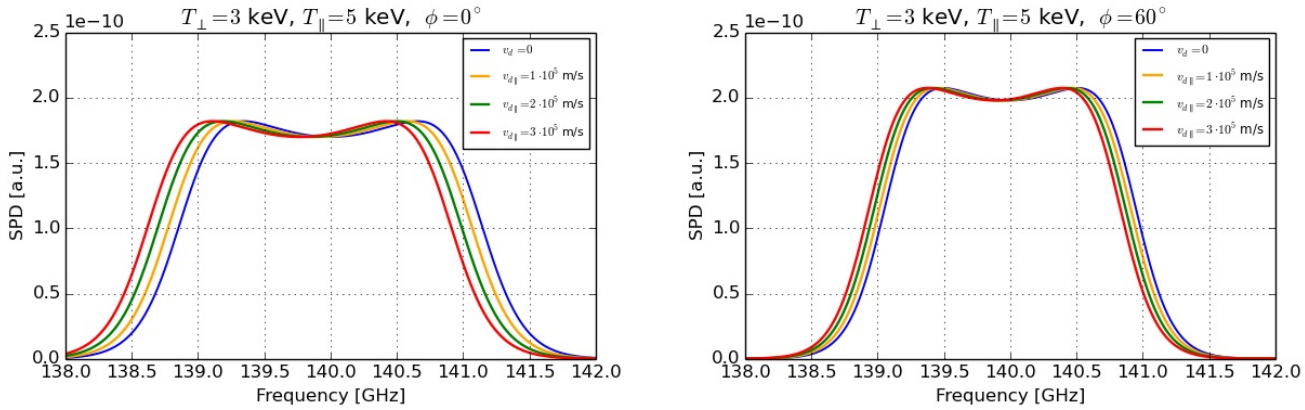

FIG. 6. Spectra computed for several parallel drift velocities and two observation angles $\phi = 0^\circ$ and $\phi = 60^\circ$. The spectral shifts caused by the parallel drift are larger for more parallel observation.